

Exciton photoluminescence of hexagonal ZnO

T. V. Butkhuzi and T. G. Chelidze

Department of Physics, Solid State Physics, Tbilisi State University, 3 Chavchavadze Avenue, Tbilisi, Georgia

A. N. Georgobiani

P. N. Lebedev Physical Institute, Academy of Sciences of Russia, Moscow, Russia

D. L. Jashiashvili, T. G. Khulordava, and B. E. Tsekvava

Department of Physics, Solid State Physics, Tbilisi State University, 3 Chavchavadze Avenue, Tbilisi, Georgia

(Received 28 January 1998; revised manuscript received 6 May 1998)

Photoluminescence spectra of ZnO layers obtained by radical-beam epitaxy have been studied. Photoluminescence of free B and C excitons has been observed. At a high excitation level a band with $\lambda_{\max} = 363.1$ nm is observed. It is explained in terms of the proposed photoluminescence polariton mechanism in the $B_{n=1}$ exciton spectral region through biexcitons [S0163-1829(98)08235-6]

I. INTRODUCTION

Exciton photoluminescence (PL) is very sensitive to the quality of crystal structures and to the presence of defects. Therefore, the regularities of the change in excitation spectra as a function of composition and structural peculiarities enable one to use them to control the quality of the crystal optically. Impurities and their associations, main lattice defects and their impurity associations, and exciton and exciton impurity complexes all play an important role in the luminescence, which significantly complicates the observation of free-exciton PL. It is apparent that the more perfect is the crystal, the more probable is the observation of free-exciton PL.

For II-VI wide-band compounds the production of exceptionally pure crystals with perfect structure is one of the most important problems. This is connected not only with the fact that reliable fundamental results can be obtained only by taking measurements on a perfect material but also with the fact that the material purity and perfection are of very great practical importance. For example, in Ref. 1 it is shown that the effective operation of laser diodes based on II-VI wide-band compounds depends strongly on the presence of point and high-dimensional defects. Growth (pre-existent) defects not only decrease the luminescence efficiency, but also cause device degradation.

In Sec. II, a method known as radical-beam epitaxy (RBE) is briefly described. This method allows one to obtain highly monocrystalline ZnO layers with a significantly reduced number of point defects. In Sec. III, PL spectra of the ZnO layers obtained by RBE with resistivities $\rho = 10^9 - 10^{11}$ and $10^{11} - 10^{13}$ Ω cm are studied.

II. RADICAL-BEAM EPITAXY

Radical-beam epitaxy enables one to obtain monocrystalline ZnO layers on the base of crystals of Zn-VI nonmetal compounds. In RBE, base crystals are treated in the atmosphere of singlet oxygen radicals. This atmosphere is created by a rf discharge. The rf oscillator converts the molecular

oxygen stream into plasma, which contains, in addition to singlet oxygen radicals, triplet oxygen radicals, oxygen ions, and electrons. An applied magnetic field causes "filtration," after which only singlet oxygen radicals reach the base crystal. Due to its activity such oxygens interact with the base crystal and form new ZnO monocrystalline layers.

The distance d between the plasma and base crystal is controlled by the magnetic field. The experiment shows that the optimal distance is $d \approx 2.5$ cm. At $d < 2.5$ cm, crystal evaporation (ion etching) takes place; at $d > 2.5$ cm there is a sharp decrease in the atomic oxygen stream falling onto the crystal surface, which reduces the efficiency of layer growth.

From the aforementioned it can be seen that RBE differs from classical epitaxy in that one component (oxygen) comes from the gaseous phase and the second component (metal) comes from the crystal bulk. The second important peculiarity of RBE is the temperature distribution in the reactor. The base crystal is in the high-temperature narrow zone of the reactor; in other parts of the reactor the temperature is much lower. Such a distribution profile removes uncontrollable impurities from the film growth zone, since they move to the low-temperature parts of the reactor. The base crystal temperature can be within 150 and 950 $^{\circ}\text{C}$. The radical concentration is $10^{14} - (5 \times 10^{15})$ cm^{-3} . In the case of thermal dissociation at $T = 1000$ K this concentration of radicals can be obtained only when the molecular oxygen pressure is $P_{\text{O}_2} = 10^6$ atm. In our case the total pressure was 0.1 atm, i.e., in the reactor the "effective pressure" from the viewpoint of a singlet oxygen radical concentration is nearly 10^7 times higher than the actual pressure. Using the RBE method, epitaxial layers with a thickness ranging from a few some atomic layers up to 50 μm can be obtained. The ZnO epitaxial layers, whose PL spectra are studied in the present work, are grown on ZnO crystals at the temperature $t = 250 - 350$ $^{\circ}\text{C}$.

III. EXCITON PHOTOLUMINESCENCE OF ZINC OXIDE

A. General conceptions

In monoaxial crystals, including II-VI compounds with a wurtzite structure, two types of dipole-permissible exciton

bands are possible: a nondegenerate exciton band of $\Gamma_1(z)$ type, and a doubly degenerate exciton band of $\Gamma_5(x,y)$ type. The expression “exciton (or electron) band of Γ_i type” means that an $E(k)$ dispersion branch is considered on which there lies a corresponding exciton term Γ_i at a zero wave vector $\vec{k}=0$ for selected wave vector directions $\vec{s}=\vec{k}/|\vec{k}|$. (Here a symmetry-caused degeneracy, but not an accidental one, is meant). The letters x,y , and z denote the representation to which wave functions of the corresponding term are transformed.

Though a number of optical phenomena in the spectral region of exciton absorption can be explained on the basis of a general theory without use of a specific exciton model and crystal types, in semiconductors a consideration based on the Wannier-Mott exciton model with allowance for exciton-photon mixing and spatial dispersion appeared to be very fruitful. In particular, on the basis of comparison of the experimental reflection spectrum near the long-wavelength edge of the fundamental absorption with the theoretical Wannier-Mott exciton model, Thomas² proposed the following scheme for the exciton spectrum in the ZnO crystal: the lowest conduction band Γ_7 and valence bands Γ_7 , Γ_9 , and Γ_7 (arranged according to their proximity to the conduction band) nearest to it form three exciton series $A(\Gamma_7 \times \Gamma_7)$, $B(\Gamma_7 \times \Gamma_9)$, and $C(\Gamma_7 \times \Gamma_7)$. The dipole-active exciton bands $\Gamma_1(z)$, and $\Gamma_5(x,y)$ are responsible for A and C series, and the $\Gamma_5(x,y)$ band is responsible for the B series.

In the spectral region of exciton absorption for dipole-active excitons, a strong interaction between the exciton and photon takes place. As a result, their dispersion laws become strongly perturbed, and there appear two new dispersion branches with excitonlike and lightlike branches corresponding to two noninteracting subsystems—exciton and photon. In the resonance region they appear as two electromagnetic-mechanical waves with radiation and mechanical energy behaviors. The conception of light-exciton mixing in the spectral region of electron exciton interactions originates from Pekar³ and Hopfield works,⁴ and the terms “exciton polariton” (or simply “polariton”) and light exciton are synonyms.⁵

It is precisely light excitons (polaritons) that are the real state of the conservative system, the crystal electromagnetic field, and this circumstance should be taken into account in the study of optical phenomena in the exciton absorption region.

In ZnO the principal state of the Wannier-Mott B exciton $B_{n=1}$ is a doubly degenerate band (at $\vec{k}\parallel\vec{C}$). For an arbitrary direction of the exciton wave vector \vec{k} the degeneracy is removed, and two excitons appear: a transverse B exciton with the exciton polarization perpendicular to the (\vec{k},\vec{C}) plane and a skew-angle B exciton with the polarization vector in the (\vec{k},\vec{C}) plane. In the spectral region of the isolated B exciton resonance from the above-mentioned excitons, two pairs of polariton modes occur due to exciton-photon mixing: (a) two branches of transverse polaritons—the upper (UPB) and lower (LPB) polariton branches with electric-field polarization perpendicular to the principal cross-section plane (\vec{k},\vec{C}) ; and (b) two branches of mixed polaritons with the polarization vector in the principal cross-section plane

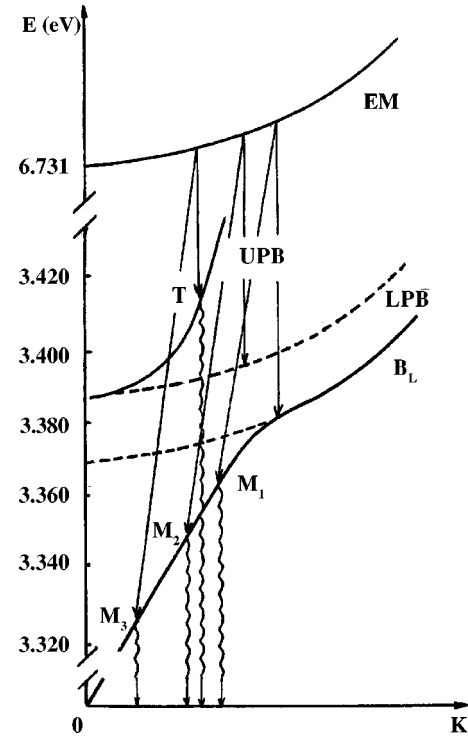


FIG. 1. Dispersion curves of excitons (dashed lines), biexcitons, and exciton polaritons in orientation $\vec{k}\perp\vec{C}$ (solid lines). The solid arrows show three channels of biexciton decay; wave arrows show radiated photons.

(\vec{k},\vec{C}) . With \vec{k} perpendicular to the optical axis \vec{C} , the mixed polariton of the lower branch transfers to a longitudinal exciton wave B_L (Fig. 1).⁶

B. Exciton photoluminescence of high-resistivity ZnO layers with $\rho=10^{11}\text{--}10^{13}\ \Omega\ \text{cm}$

High-resistivity ZnO layers of $\approx\mu\text{m}$ thickness obtained by RBE on the basis of ZnO monocrystals with a resistivity $\rho\approx 10^{11}\text{--}10^{13}\ \Omega\ \text{cm}$ were excited by nitrogen laser radiation ($\lambda=337$ and $1\ \text{nm}$) at liquid-nitrogen temperature $T=77\ \text{K}$. It is remarkable that in the complete absence of visible luminescence, intensive bands with $\lambda_{\text{max}}=367.7\ \text{nm}$, $\lambda_{\text{max}}=366.8\ \text{nm}$, and $\lambda_{\text{max}}=362.7\ \text{nm}$ were observed. The half-widths of these bands were, respectively, $\Delta E=6\ \text{meV}$ for $\lambda_{\text{max}}=362.7\ \text{nm}$ and $\Delta E=10\text{--}12\ \text{meV}$ for the bands $\lambda_{\text{max}}=367.7\ \text{nm}$ and $\lambda_{\text{max}}=366.8\ \text{nm}$ (Fig. 2 curve a).

Due to the proximity of these bands to each other, it is difficult to define an individual half-width for each band. To establish their nature, the luminescence polarization was measured. According to x-ray investigations, the hexagonal axis is perpendicular to the film surface. In spite of the fact that such an axis orientation causes some difficulties in measuring the polarization, a marked difference in the dependence of the luminescence band intensity on light polarization was established. The band with $\lambda_{\text{max}}=366.8\ \text{nm}$ had a pronounced intensity dependence on polarization in contrast to the bands with $\lambda_{\text{max}}=362.7$ and $367.7\ \text{nm}$ (Fig. 2 curve a'). This difference allows one to distinguish closely spaced bands with the maxima $\lambda=366.8$ and $367.7\ \text{nm}$. The spectral

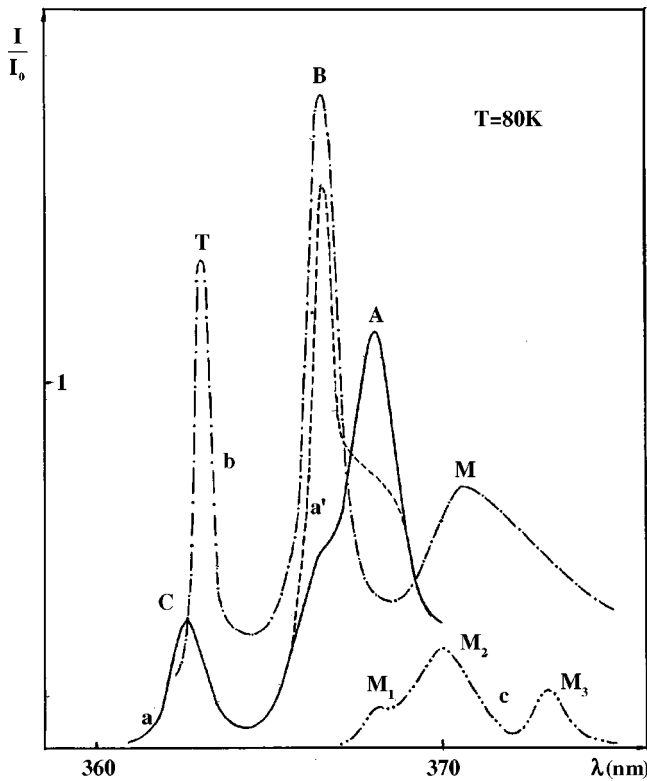


FIG. 2. PL spectra of ZnO layers: curve a — $\rho = 10^{11}$ – 10^{13} Ω cm; curve a' — $\rho = 10^{11}$ – 10^{13} Ω cm; $\vec{k} \perp \vec{C}$; curve b — $\rho = 10^9$ – 10^{10} Ω cm; curve c —structure of the M band.

arrangement of these bands coincides with the free-exciton energies in the reflection spectra. Therefore we think that radiative recombination of free A —($\lambda_{\max} = 367.7$ nm), B —($\lambda_{\max} = 366.8$ nm) and C —($\lambda_{\max} = 367.7$ nm) excitons is observed. It is believed that short-wavelength B and C excitons cannot be seen in the luminescence, primarily due to strong reabsorption and thermalization processes (i.e., the processes bringing an exciton to temperature equilibrium with the lattice).

Since the energy gap between A and B excitons, $E_{AB} = 8$ meV, is of the order of liquid-nitrogen temperature, 6.7 meV, the thermalization channel cannot lead to a strong difference in A - and B -exciton concentrations. As for degradation from C -exciton energy levels, the energy difference is $E_{AC} = 48$ meV and $E_{BC} = 40$ meV. However, since in polar semiconductors the most probable interaction is the one with longitudinal-optical phonons, and the longitudinal-optical-phonon energy is $E_{LO} = 72$ meV, this degradation channel is improbable.

Thus, in the absence of defects, the radiative degradation is improbable. As for B - and C -exciton degradation due to hole transfers to the valence subbands, this process should be accompanied by infrared quantum radiation with the wavelengths $\lambda_{\max} = 25.8$ and 31.0 μm , which are not observed in the spectrum. There are various mechanisms determined by crystal structure defects which cause radiation “death” of free excitons.

(1) Free-exciton dissociation into the electron-hole pair in the electric field of charged defects.

(2) Exciton annihilation followed by transmission of the energy of radiative transition to the electron trapped by the

defects, which is ejected into the conductive band, and at consequent thermalization gives a part of its energy to the crystal lattice.

(3) Excitons can bind to impurities or defects forming bound-exciton states (exciton-impurity complexes, multiexciton-impurity complexes, etc.).

Observation of short-wavelength B and C excitons in these samples shows that the radiative recombination prevails over the processes of non-radiative energy degradation.

The absence of visible luminescence and observation of free excitons in a thin near-surface region shows that ZnO layers obtained by RBE are characterized by high purity and perfection of the crystal lattice. The high resistivity of the samples under investigation is presumably due to a low structural defect concentration rather than to self-compensation, since bound-exciton bands as well as the visible spectrum band would be expected in the PL spectra in the latter case.

C. Exciton luminescence of ZnO layers with $\rho = 10^9$ – 10^{11} Ω cm at a high excitation level

The characteristic features of these layers are the actual absence of visible luminescence and the presence of pronounced exciton bands in the ultraviolet region. As seen in Fig. 2(b) three bands with maxima $\lambda = 363.1$ nm (3.412 eV), $\lambda = 366.8$ nm (3.378 eV), and $\lambda = 370.6$ nm (3.343 eV) are observed. The comparison of these bands with the reflection spectra enables one to ascribe the band with $\lambda_{\max} = 366.8$ nm to free B -exciton radiation.

The radiation band with a maximum at $\lambda = 363.1$ nm (T band) is reported for the first time, to the best of our knowledge. The band with the maximum $\lambda = 370.7$ nm is known in the literature as the M band, and is interpreted in different ways. Some authors regard it as a result of the interaction of a free exciton with electrons,⁷ some as radiative decay of a biexciton,^{8,9} while others regard it as electron-hole plasma recombination.¹⁰

The M band appears at low temperatures and at a high excitation level. The characteristic feature of this band is an asymmetric shape and an extended long-wavelength wing. At $T = 80$ K and a pumping intensity $I = 10^{14}$ w/cm² in the M -band spectrum, there appears a structure with three maxima which are denoted in Fig. 2(c) as M_1 ($\lambda = 368.5$ nm, 3.362 eV), M_2 ($\lambda = 370.0$ nm, 3.348 eV), and M_3 ($\lambda = 373.0$ nm, 3.322 eV). With the pumping intensity increase the M -band structure disappears, and its maximum is shifted toward the long-wavelength side of the spectrum.

Simultaneous observation of the M and T bands in the PL spectrum gave grounds to take the biexciton version of M -band occurrence. At strong band-to-band layer excitation ($\lambda = 337.1$ nm), a large number of excitons are created in crystal. In this system of high density of excitons, exciton molecules (EM's) thermalized in their ground state Γ_1 with the orbital momentum $J_{EM} = 0$ are treated.

According to the selection rules dipole-permissible transitions ($\Delta J = \pm 1$) from the biexciton ground state $J = 0$ transitions to exciton-polariton states of transverse and mixed branches are possible (in a particular case of the exciton wave vector $\vec{k} \perp \vec{C}$ to the states of purely longitudinal B_L

TABLE I. Results for free-exciton radiation bands.

A exciton	367.7 nm	3.369 eV				
			M_1	368.5 nm	3.362 eV	
B exciton	366.8 nm	3.378 eV	LPB	M_2	370.0 nm	3.348 eV
				M_3	373.0 nm	3.322 eV
			UPB	T	363.1 nm	3.412 eV
C exciton	362.7 nm	3.416 eV				

exciton). The obtained experimental spectra can be explained by the presence of the following three channels of exciton molecule decay.

(1) As a result of the EM decay a lightlike state M_1 of the LPB and an excitonlike state of the LPB are formed. On reaching the crystal surface the lightlike polariton escapes as a luminescence photon M_1 ($\lambda = 368.5$ nm, 3.362 eV).

(2) The exciton molecule causes a lightlike state of the LPB and a longitudinal exciton state B_L . Reaching the crystal surface the lightlike polariton escapes as a photon M_2 ($\lambda = 370.0$ nm, 3.348 eV).

(3) The EM decay results in the appearance of two lightlike polaritons of the lower and upper branches. Both polari-

tons reach the crystal surface and escape as photons M_3 ($\lambda = 373.0$ nm, 3.322 eV) and T ($\lambda = 363.1$ nm, 3.412 eV).

Thus the T band is ascribed to radiation of a polariton of the upper branch. The exciton molecule energy in ZnO is within $6.7310 < E_{EM} < 6.740$ eV, which corresponds to the interval $362.49 \leq \lambda_{UPB} \leq 363.49$ nm for the wavelength of radiation from the upper polariton branch. The obtained λ_{UPB} value is in perfect agreement with the T -band position (363.1 nm). In this frequency range the upper polaritons have a relatively high group velocity $V_g(\vec{k})$ and an average free-path length $L(\vec{k})$; therefore the polariton can easily reach the surface and escape from the crystal.

The presence of free-exciton radiation bands in photoluminescence spectra and the absence of visible luminescence suggest that the ZnO films are characterized by a high structural perfection up to the thin near-surface region and a negligible content of uncontrollable defects and impurities. The obtained results are given in Table I.

ACKNOWLEDGMENT

The authors would like to express their sincere thanks to the International Science Foundation for providing a grant.

¹A. Isibashi, M. Ukita, and S. Tomiya, in *Proceedings of the 23rd International Conference on the Physics of Semiconductors, Berlin, Germany, July 21-26, 1996* (World Scientific, Singapore, 1996), Vol. 4, pp. 3155–3162.

²D. G. Thomas, *J. Phys. Chem. Solids* **15**, 86 (1960).

³S. I. Pekar, *Zh. Éksp. Teor. Fiz.* **33**, 1022 (1957) [*Sov. Phys. JETP* **6**, 785 (1985)].

⁴J. J. Hopfield, *Phys. Rev.* **112**, 1555 (1958).

⁵S. I. Pekar, *Zh. Éksp. Teor. Fiz.* **38**, 1786 (1960) [*Sov. Phys.*

JETP **38**, 1786 (1960)].

⁶A. A. Demidenko, S. I. Pekar, and B. E. Tsekvava, *Zh. Éksp. Teor. Fiz.* **76**, 1445 (1979) [*Sov. Phys. JETP* **76**, 1455 (1979)].

⁷G. Klinghirn, *Phys. Status Solidi B* **73**, 587 (1975).

⁸J. Segawa and S. Namba, *J. Lumin.* **12/13**, 589 (1976).

⁹J. M. Hvam, *Phys. Status Solidi B* **93**, 581 (1976).

¹⁰V. A. Korneitchuk and M. K. Sheikman, *Fiz. Tverd. Tela (Leningrad)* **22**, 1534 (1980) [*Sov. Phys. Solid State* **22**, 1534 (1980)].